JOURNAL OF SOLID STATE CHEMISTRY **121,** 133–137 (1996)
ARTICLE NO. 0019

# Preparation and the Crystal Structure of Ten-Layer $Ba_5Fe_4NiO_{13.5}$

H. Takizawa[1,2] and H. Steinfink

*Department of Chemical Engineering, The University of Texas at Austin, Austin, Texas 78712-1062*

Received March 13, 1995; revised June 30, 1995; accepted August 2, 1995

**$Ba_5Fe_4NiO_{13.5}$ ($BaFe_{0.8}Ni_{0.2}O_{2.70}$) was synthesized by heating the mixed nitrates at 700°C for 72 h in air. The crystal structure has been analyzed by Rietveld analysis of the powder X-ray diffraction data. $Ba_5Fe_4NiO_{13.5}$ has a hexagonal unit cell, space group $P6_3/mmc$ with lattice parameters $a = 5.7713(3)$ Å and $c = 24.5812(16)$ Å. The structure is formed by the stacking of 10 close-packed $BaO_3$ layers consisting of six hexagonal and four cubic sequences. This stacking creates trinuclear and binuclear face sharing octahedral units that are linked by corner sharing into a column approximately 24-Å high. The Ni ion preferentially occupies the central octahedral interstice of the trinuclear unit and the Fe ions occupy all the other sites. The interatomic distances and the result of a magnetic measurement are consistent with the presence of 50% high-spin $Fe^{4+}$, 50% high-spin $Fe^{3+}$, and low-spin $Ni^{3+}$ states.** 

## INTRODUCTION

The crystal structures of perovskite related compounds $ABO_3$, where $A$ is a large cation like Ba or Sr and $B$ is a transition metal ion, are described in terms of close packing of $AO_3$ layers with $B$ cations occupying interlayer octahedral sites. The $AO_3$ layers are stacked hexagonally and/or cubically, and this generates theoretically a large number of unique structures depending on the number of layers and the stacking sequences (1). The cubic stacking of $AO_3$ layers leads to the formation of corner sharing octahedra and the hexagonal stacking leads to face sharing octahedra.

In $BaMO_3$ ($M$ = transition metal), various representations of the close-packed structures have been reported. $BaTiO_3$ (2) has a hexagonal six-layer structure with the stacking sequence *hchhhc* where *h* and *c* denote hexagonal and cubic layers. $BaMnO_3$ (3) has a hexagonal four-layer structure with the sequence $(hc)_2$; near stoichiometric $BaFeO_3$ is reported to be cubic with the *ccc* arrangement (4), but the structures of nonstoichiometric, oxygen deficient, phases exhibit complex stacking sequences (5, 6); $BaNiO_3$ (7) is hexagonal two-layer, *hh*; $BaRuO_3$ (8) is rhombohedral nine-layer, $(hhc)_3$. Other stacking sequences are reported in $BaMnO_{3-x}$ (9, 10) and $Ba(Ir_{1-x}Co_x)O_{3-y}$ (11).

It was reported that the bond nature between $M$ and O ions, as well as the size of the transition metal ion relative to the $A$ cation and O, is an important factor in determining the stacking sequence in $BaMO_3$ (7). In addition, the ordering between transition metal ions may cause various stacking sequences in mixed transition metal system, $Ba(M, M)O_3$.

In the present study, a new 10-layer phase, $Ba_5Fe_4NiO_{15-\delta}$ has been synthesized and the crystal structure has been analyzed by the Rietveld method.

## EXPERIMENTAL

$Ba_5Fe_4NiO_{13.5}$ ($BaFe_{0.8}Ni_{0.2}O_{2.70}$) was synthesized through the nitrate route. Reagent grade $Ba(NO_3)_2$, $Fe(NO_3)_3 \cdot 9H_2O$), and $Ni(NO_3)_2 \cdot 6H_2O$ were used as starting materials. These nitrates were carefully weighed in molar ratios $Ba:Fe:Ni = 1:1 - x:x$ and dissolved in distilled water.

After evaporation to dryness, the mixed nitrates were gently heated to 600°C and kept at this temperature for 2 hr. The resulting black powders were heated at 700°C for 72 hr in air and slowly cooled to room temperature. A single phase product was obtained only at $x = 0.2$ as an intermediate phase in $(1 - x)BaFeO_{3-\delta}$–$xBaNiO_{3-\delta}$ with composition $BaFe_{0.8}Ni_{0.2}O_{3-\delta}$.

The product was analyzed by X-ray powder diffraction using a diffractometer fitted with a graphite monochromator and Cu$K\alpha$ radiation. The crystal structure was solved by the Rietveld analysis of the powder X-ray diffraction data using the RIETAN program written by Izumi (12). The diffraction data were collected at room temperature by step scan over an angular range $5° < 2\theta < 140°$ with the step increment of 0.04° and counting time of 5 sec. The oxygen content of the compound was determined by iodometric titration (13).

[1] Permanent address: Department of Molecular Chemistry and Engineering, Tohoku University, Sendai, Miyagi 980-77, Japan.

[2] To whom correspondence should be addressed.



0022-4596/96 $12.00

## RESULTS AND DISCUSSION

Single phase $Ba_5Fe_4NiO_{15-\delta}$ was obtained after the reaction at 700°C for 72 hr. The X-ray powder diffraction data were completely indexed on the basis of a hexagonal unit cell with preliminary lattice parameters $a = 5.771(1)$ Å and $c = 24.58(3)$ Å. The value of the $a$ axis is in good agreement with the value for the close-packed dimension in a $BaO_3$ layer. The length of the $c$ axis corresponds to 10 times the thickness of a $BaO_3$ layer (2.3 to 2.45 Å) suggesting the compound has a 10-layer stacking of close-packed $BaO_3$ layers. The oxidation states of transition metal ions were determined to be $M^{3+}_{0.597}M^{4+}_{0.403}$, which corresponds to the chemical composition of $Ba_5Fe_4NiO_{13.5}$. The observed and calculated diffraction data are listed in Table 1.

The crystal structure was determined by the Rietveld analysis of the powder X-ray diffraction data using 660 reflections. The International Tables for X-ray Crystallography (14) list three possible 10-layer stacking sequences for the only suitable group $P6_3/mmc$ as described by Negas and Roth (9). These are |(5)|(5)|, |1(3)1|1(3)1|, and |2(1)2|2(1)2| in Zhdanov notation, corresponding to 80% cubic stacking and 20% hexagonal stacking as $(hcccc)_2$, 40% cubic stacking and 60% hexagonal stacking as $(hhhcc)_2$, and 40% cubic stacking and 60% hexagonal stacking as $(hchhc)_2$, respectively. The |(5)|(5)| stacking was reported for $Ba_5W_3LiO_{14.5}$ (15) and the |2(1)2|2(1)2| stacking was found in $BaMnO_{3-x}$ (9) and $BaIr_{0.3}Co_{0.7}O_{2.83}$ (11). Structural analysis was carried out for these three possible stacking sequences. The best result was obtained for the |2(1)2|2(1)2| stacking sequence. The other stacking sequences gave $R$ values greater than 30%. The stacking sequence consists of triplets of face-sharing octahedra connected by corner sharing with two face-sharing octahedra. Twenty percent of the transition metal ions are located in face-sharing octahedra and the others are in the octahedra sharing both corners and faces.

Table 2 lists the atomic coordinates for $Ba_5Fe_4NiO_{13.5}$. The oxygen vacancy distribution was assumed to be random for the calculation, i.e., the occupation factors of O(1), O(2), and O(3) were fixed at 0.90. Several different models for the oxygen distribution were tried but the $R$ values for the different refinements did not differ significantly. Figure 1 shows the observed and calculated X-ray diffraction patterns and the difference profile for $Ba_5Fe_4NiO_{13.5}$. The final reliability factors are $R_{wp} = 16.82\%$, $R_1 = 7.37\%$, and $R_F = 4.22\%$, where $R_{wp}$, $R_1$, and $R_F$, are the reliability factors for the weighted pattern, integrated intensity, and structure factor, respectively. The two Ni atoms were placed in 2$a$ sites of the space group and thus occupy the face-sharing octahedral sites; the Fe atoms are in the 4$f$ positions and occupy the interstices of the octahedra sharing both corners and faces. This distribution suggests a

**TABLE 1**

**The Observed and Calculated X-Ray Diffraction Data for $Ba_5Fe_4NiO_{13.5}$**

| $h$ | $k$ | $l$ | $d_{obs.}$ | $d_{calc.}$ | $I_{obs.}$ | $I_{calc.}$ |
|---|---|---|---|---|---|---|
| 0 | 0 | 2 | 12.34 | 12.290 | 6 | 11 |
| 1 | 0 | 2 | 4.635 | 4.630 | 4 | 8 |
| 1 | 0 | 4 | 3.881 | 3.877 | 9 | 9 |
| 1 | 0 | 5 | 3.508 | 3.505 | 27 | 34 |
| 1 | 0 | 6 | 3.171 | 3.168 | 11 | 13 |
| 0 | 0 | 8 | 3.075 | 3.073 | 5 | 6 |
| 1 | 1 | 0 | 2.883 | 2.886 | 100 | 100 |
| 1 | 0 | 7 | 2.875 | 2.873 | 54 | 54 |
| 1 | 0 | 8 | 2.619 | 2.618 | 9 | 8 |
| 2 | 0 | 0 | 2.500 | 2.499 | 2 | 5 |
| 0 | 0 | 10 | 2.460 | 2.458 | 6 | 5 |
| 2 | 0 | 2 | 2.447 | 2.449 | 3 | 7 |
| 2 | 0 | 4 | 2.316 | 2.315 | 4 | 6 |
| 2 | 0 | 5 | 2.229 | 2.228 | 35 | 34 |
| 2 | 0 | 6 | 2.135 | 2.133 | 9 | 9 |
| 1 | 1 | 8 | 2.105 | 2.103 | 19 | 13 |
| 2 | 0 | 7 | 2.034 | 2.036 | 33 | 29 |
| 2 | 0 | 8 | 1.940 | 1.939 | 5 | 7 |
| 1 | 0 | 12 | 1.896 | 1.895 | 12 | 10 |
| 1 | 1 | 10 | 1.871 | 1.871 | 5 | 8 |
| 2 | 1 | 2 | 1.868 | 1.867 | 2 | 2 |
| 1 | 0 | 13 | 1.769 | 1.768 | 6 | 5 |
| 2 | 1 | 5 | 1.764 | 1.763 | 11 | 9 |
| 0 | 0 | 14 | 1.757 | 1.756 | 3 | 2 |
| 2 | 1 | 6 | 1.713 | 1.715 | 5 | 4 |
| 1 | 1 | 12 | 1.671 | 1.670 | 6 | 5 |
| 3 | 0 | 0 | 1.667 | 1.666 | 25 | 23 |
| 2 | 1 | 7 | 1.664 | 1.664 | 27 | 24 |
| 2 | 1 | 8 | 1.610 | 1.609 | 6 | 5 |
| 2 | 0 | 12 | 1.582 | 1.584 | 9 | 8 |
| 2 | 0 | 13 | 1.508 | 1.508 | 4 | 2 |
| 1 | 1 | 14 | 1.500 | 1.500 | 13 | 9 |
| 2 | 1 | 10 | 1.498 | 1.498 | 4 | 1 |
| 3 | 0 | 8 | 1.465 | 1.464 | 5 | 3 |
| 2 | 2 | 0 | 1.443 | 1.443 | 9 | 10 |
| 1 | 0 | 17 | 1.389 | 1.389 | 5 | 3 |
| 2 | 1 | 12 | 1.388 | 1.388 | 10 | 8 |
| 2 | 0 | 15 | 1.370 | 1.370 | 2 | 1 |
| 1 | 1 | 16 | 1.356 | 1.356 | 4 | 2 |

**TABLE 2**

**Atomic Coordinates for $Ba_5Fe_4NiO_{13.5}$**

Space group: $P6_3/mmc$ (No. 194); $a = 5.7713(3)$ Å, $c = 24.5812(16)$ Å

| Atom | Position | $x$ | $y$ | $z$ | $B$ (Å$^2$) |
|---|---|---|---|---|---|
| Ba(1) | 2$b$ | 0 | 0 | 1/4 | 0.5(2) |
| Ba(2) | 4$f$ | 1/3 | 2/3 | 0.1270(3) | 0.8(3) |
| Ba(3) | 4$f$ | 1/3 | 2/3 | 0.5380(3) | 0.3(2) |
| Fe(1) | 4$f$ | 1/3 | 2/3 | 0.6814(9) | 0.6(1) |
| Fe(2) | 4$e$ | 0 | 0 | 0.1091(6) | 0.6(1) |
| Ni | 2$a$ | 0 | 0 | 0 | 0.5(1) |
| O(1) | 6$h$ | 0.522(3) | 0.044 | 1/4 | 1.9(3) |
| O(2) | 12$k$ | 0.157(3) | 0.314 | 0.047(2) | 1.3(3) |
| O(3) | 12$k$ | 0.8297(16) | 0.6594 | 0.1502(9) | 0.9(2) |

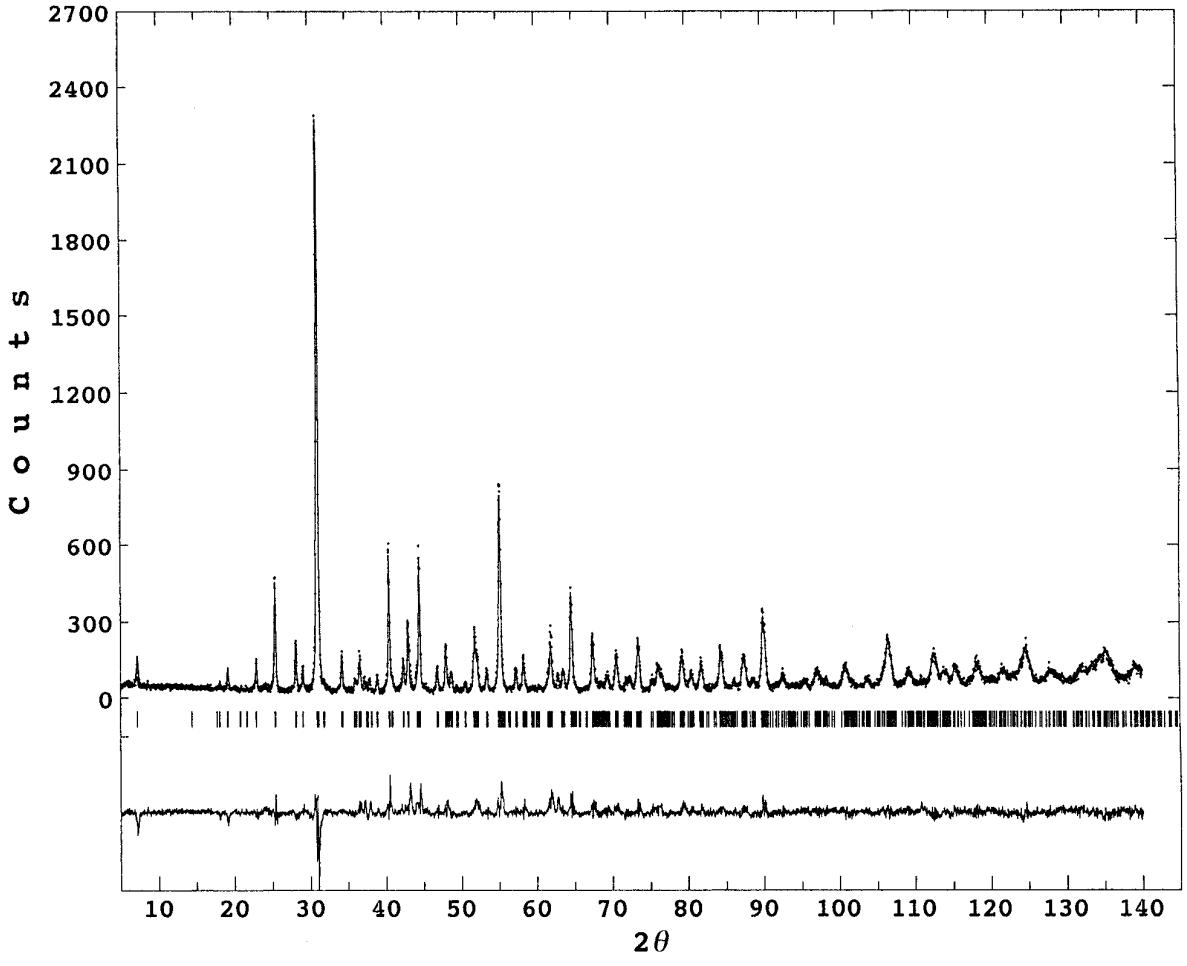


**FIG. 1.** X-ray Rietveld refinement profile for $Ba_5Fe_4NiO_{13.5}$. Points are the raw data and the solid line is the calculated profile. Tick marks below the profile show the allowed reflections. A difference curve, observed-calculated, is plotted beneath.

fixed composition $Ba_5Fe_4NiO_{13.5}$ for the compound, rather than a solid solution $BaFe_{1-x}Ni_xO_{3-\delta}$ and is consistent with the synthetic result. This preferential distribution of the transition metal atoms is also compatible with the fact that Ni atoms have a strong tendency to stabilize face-sharing structures as observed in $BaNiO_3$ (7) and $SrNiO_{3-x}$ (16). The idealized crystal structure including the arrangement of octahedra is shown in Fig. 2.

The interatomic distances and bond angles are given in Table 3. The Ba–O and O–O distances within the $BaO_3$ layers are in the range 2.72–3.04 Å except 2.50(3) Å for O(1)–O(1). In the idealized close-packed stacking of $BaO_3$ layers all the Ba–O and O–O distances within the layers and between adjacent layers should be the same, nearly equal to 2.9 Å from the ionic radii (17). However, the Ba–O and O–O distances between adjacent layers are widely distributed in the range 2.63–3.56 Å. Such flexible packing is considered to be due to the large amount of oxygen vacancies.

The local environment of transition metal atoms is shown in Fig. 3. The $NiO_6$ octahedra, consist of six identical Ni–O bonds, 1.955(12) Å, and are quite regular. This interatomic distance is in good agreement with the sum of the ionic radii, 1.96 Å for low-spin $Ni^{3+}$ ($3d^7$). The $FeO_6$ octahedra are rather distorted, especially for $Fe(1)O_6$. This considerable distortion suggests a high concentration of oxygen vacancies in the hexagonal layers. Assuming that all Ni ions are in the trivalent state, half of the Fe ions should be $Fe^{4+}$ ($3d^4$) and half $Fe^{3+}$ ($3d^5$). The Fe–O distances from ionic radii are 2.00 Å (high-spin $Fe^{4+}$) and 2.05 Å (high-spin $Fe^{3+}$) for octahedral coordination. The short Fe(1)–O(3) distances in the $Fe(1)O_6$ octahedra suggest the possible existence of tetrahedral coordination. The average distance in $FeO_4$ tetrahedra is reported to be 1.87 Å in $SrFeO_{2.5}$ (16) and 1.88 Å in $Ca_2Cr_{0.5}Fe_{1.5}O_5$ (17).

The O(1)–O(1) distances in a hexagonal layer are 2.50(3) Å. This value is considerably less than the sum of the ionic radii. Such a shortening is considered to be due

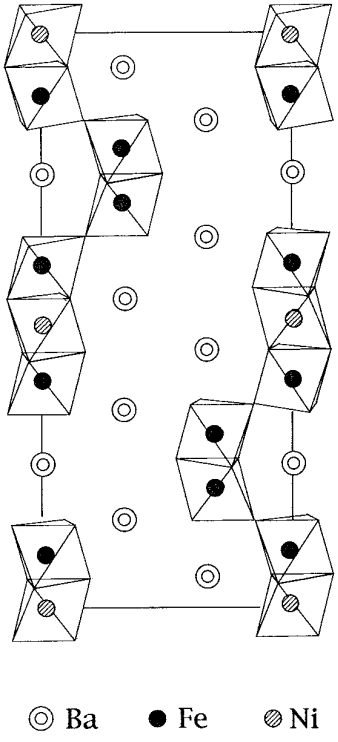


**FIG. 2.** Projection of the structure of $Ba_5Fe_4NiO_{13.5}$ on ($h0l$).

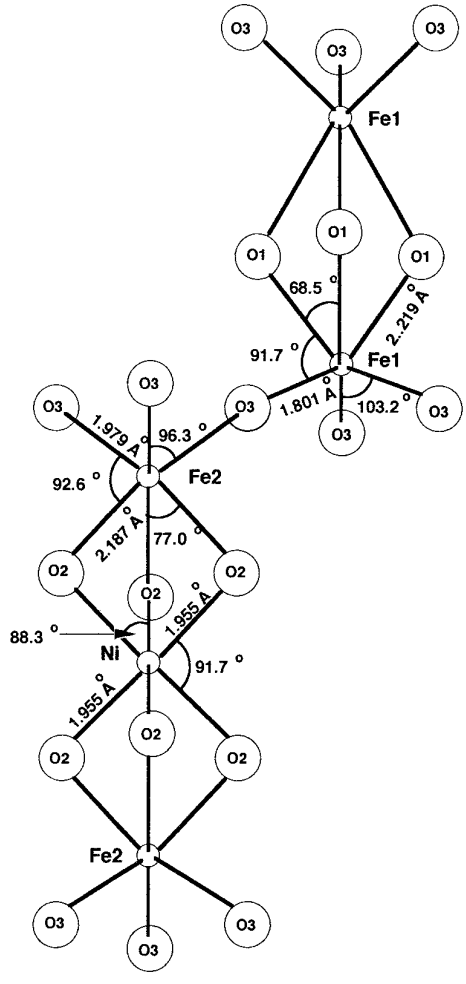


**FIG. 3.** Bond lengths and angles for the structural units in $Ba_5Fe_4NiO_{13.5}$.

**TABLE 3**
**Interatomic Distances (Å) and Bond Angles (°) for $Ba_5Fe_4NiO_{13.5}$**

| | | | | | |
|---|---|---|---|---|---|
| Ba(1)–O(1) | 2.894(16) | 6× | O(1)–O(1) | 2.50(3) | 2× |
| –O(3) | 2.986(4) | 6× | –O(1) | 3.272(12) | 2× |
| Ba(2)–O(1) | 3.564(12) | 3× | –O(3) | 2.899(11) | 4× |
| –O(2) | 2.63(2) | 3× | O(2)–O(2) | 2.72(3) | 2× |
| –O(3) | 2.942(8) | 6× | –O(2) | 2.806(9) | 2× |
| Ba(3)–O(2) | 2.73(2) | 3× | –O(2) | 3.048(15) | 2× |
| | 2.896(3) | 6× | –O(3) | 3.01(3) | 2× |
| –O(3) | 3.20(2) | 3× | O(3)–O(3) | 2.82(3) | 2× |
| Fe(1)–O(1) | 2.219(15) | 3× | –O(3) | 2.949(11) | 1× |
| –O(3) | 1.801(12) | 3× | Ni–Fe(2) | 2.683(16) | 2× |
| Fe(2)–O(2) | 2.187(15) | 3× | | | |
| –O(3) | 1.979(11) | 3× | | | |
| Ni–O(2) | 1.955(12) | 6× | | | |

Angles

| | | | |
|---|---|---|---|
| O(1)–Fe(1)–O(1) | 68.5(6) | O(2)–Ni–O(2) | 88.3(3) |
| O(1)–Fe(1)–O(3) | 91.7(5) | O(2)–Ni–O(2) | 91.7(4) |
| O(1)–Fe(1)–O(3) | 155.8(6) | O(2)–Ni–O(2) | 180.0(0) |
| O(3)–Fe(1)–O(3) | 103.2(6) | Fe(1)–O(1)–Fe(1) | 98.9(8) |
| O(2)–Fe(2)–O(2) | 77.0(6) | Fe(1)–O(3)–Fe(2) | 174.5(9) |
| O(2)–Fe(2)–O(3) | 92.6(4) | Fe(2)–O(2)–Ni | 80.5(7) |
| O(2)–Fe(2)–O(3) | 166.6(9) | | |
| O(3)–Fe(2)–O(3) | 96.3(5) | | |

to the high concentration of oxygen vacancies as was observed in 4H $Ba_{0.5}Sr_{0.5}MnO_{2.83}$ (2.471 Å) (20) and 6H Ba $FeO_{2.79}$, (2.448 Å) (21). This, as well as the distortion of the Fe(1) octahedra and the large value of the O1 displacement parameter, support the preferential distribution of oxygen vacancies in the O(1) site, although no significant changes in $R$ factors were observed in the Rietveld refinement as mentioned previously. It should be noted that Jacobson (19) reported the unequal distribution of O vacancies in 6H $BaFeO_{2.79}$, from a neutron diffraction study; the hexagonal layers have the composition $BaO_{2.5}$ and the cubic layers $BaO_{2.835}$.

The magnetic susceptibility was measured in the temperature range 4.2–300 K using a SQUID magnetometer at a magnetic field of 1 kOe. Figure 4 shows the temperature dependence of the inverse magnetic susceptibility of $Ba_5Fe_4NiO_{13.5}$. The magnetic susceptibility was fit to the Curie–Weiss type relation; $\chi = C/(T - T_0) + \chi_c$, where

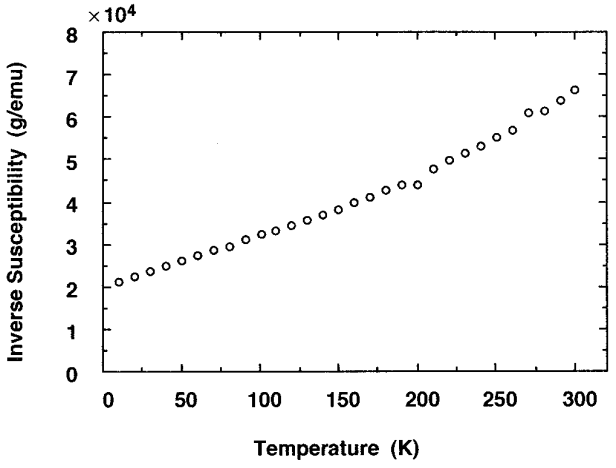


**FIG. 4.** Inverse magnetic susceptibility vs temperature for $Ba_5Fe_4NiO_{13.5}$.

$C$, $T_0$, and $\chi_c$ are the Curie constant, the Curie–Weiss constant, and the temperature independent susceptibility, respectively. The parameters $C$, $T_0$, and $\chi$ were determined by a least squares fit as 3.72, −255 K, and $-3.05 \times 10^{-5}$ emu/mole for the chemical formula $BaFe_{0.8}Ni_{0.2}O_{2.7}$. The negative value of $T_0$ indicates antiferromagnetic interaction between transition metal atoms in this material. The effective magnetic moment per transition metal atom was calculated to be 5.45(3) $\mu_B$. This value is comparable with the estimated value, 4.92 $\mu_B$, by the spin-only approximation for 40% high-spin $Fe^{3+}$ ($t_{2g}^3e_g^2$), 40% high-spin $Fe^{4+}$ ($t_{2g}^3e_g^1$), and 20% low-spin $Ni^{3+}$ ($t_{2g}^6e_g^1$). This suggested valence distribution is based on structural and crystal chemical considerations. The magnetic data can be reconciled with other valence models and a detailed Mössbauer study would be needed to determine this aspect of the compound.

## SUMMARY

A new 10-layer compound with chemical formula $Ba_5Fe_4NiO_{13.5}$ has been synthesized by codecomposition of mixed nitrates. The compound consists of both hexagonal and cubic stacking of $BaO_3$ layers with the sequence $(hchhc)_2$. The interatomic distances show a preferential distribution of oxygen vacancies in the hexagonal layer formed by O(1). The $M$–O bond lengths ($M$ = transition metal) suggest a cation valence distribution of $Ba_5Fe_2^{III}Fe_2^{IV}Ni^{III}O_{13.5}$. The ordering between transition metal atoms in octahedral sites suggests possible occurrences of new phases with different stacking sequences of $BaO_3$ layers in other combinations of transition metal atoms.

## ACKNOWLEDGMENTS

H.T. gratefully acknowledges the support by an Overseas Research Program of the Ministry of Education, Science, and Culture, Japan. H.S. acknowledges the support of the R.A. Welch Foundation, Houston, Texas. The authors are indebted to Dr. J. T. Markert, Professor of Physics, University of Texas, Austin, Texas, for the magnetic measurement.

## REFERENCES

1. Katz, L., and Ward, R., *Inorg. Chem.* **3,** 305 (1964).
2. Burbank, R. D., and Evans, H. T., *Acta Crystallogr.* **1,** 330 (1948).
3. Hardy, A., *Acta Crystallogr.* **15,** 179 (1962).
4. Derbyshire, S. W., Fraker, A. C., and Stadelmaier, H. H., *Acta Crystallogr.* **14,** 1293 (1961).
5. Grenier, J.-C., Wattiaux, A., Pouchard, M., Hagenmuller, P., Parras, M., Vallet, M., Calbet, J., and Alario-Franco, M. A., *J. Solid State Chem.* **80,** 6 (1989).
6. Parras, M., Vallet-Regi, M., Gonzalez-Calbet, J. M., and Grenier, J. C., *J. Solid State Chem.* **83,** 121 (1989).
7. Takeda, Y., Kanamaru, F., Shimada, M., and Koizumi, M., *Acta Crystallogr. Sect. B* **32,** 2464 (1976).
8. Donohue, P. C., Katz, L., and Ward, R., *Inorg. Chem.* **4,** 306 (1965).
9. Negas, T., and Roth, R. S., *J. Solid State Chem.* **3,** 323 (1971).
10. Parras, M., Gonzalez-Calbet, J. M., Alonso, J., and Vallet-Regi, M., *J. Solid State Chem.* **113,** 78 (1994).
11. Schaller, H. U., Kemmler-Sack, S., and Ehmann, A., *J. Less-Common Met.* **97,** 299 (1984).
12. Izumi, F., *in* "The Rietveld Method" (R. A. Young, Ed.), Chap. 13. Oxford Univ. Press, Oxford, 1993.
13. Day, R. A., Jr., and Underwood, A. L., Quantitative Analysis" 4th ed., Chap. 11. Prentice-Hall, New Jersey, 1980.
14. "International Tables for X-ray Crystallography" Vol. II, p. 342. Kynoch Press, Birmingham, UK, 1959.
15. Jendrek, E. F., Jr., Potoff, A. D., and Katz, L., *J. Solid State Chem.* **14,** 165 (1975).
16. Takeda, Y., Hashino, T., Miyamoto, H., Kanamaru, F., Kume, S., and Koizumi, M., *J. Inorg. Nucl. Chem.* **34,** 1599 (1972).
17. Shannon, R. D., *Acta Crystallogr. Sect. A* **32,** 751 (1976).
18. Greaves, C., Jacobson, A. J., Tofield, B. C., and Fender, B. E. F., *Acta Crystallogr. Sect. B* **31,** 641 (1975).
19. Battle, P. D., Bollen, S. K., Gibb, T. C., and Matsuo, M., *J. Solid State Chem.* **90,** 42 (1991).
20. Potoff, A. D., Chamberland, B. L., and Katz, L., *J. Solid State Chem.* **8,** 234 (1973).
21. Jacobson, A. J., *Acta Crystallogr. Sect. B* **32,** 1087 (1976).